第 15 卷　第 12 期
2007 年 12 月

光学 精密工程
Optics and Precision Engineering

Vol. 15　No. 12
Dec. 2007

Article ID　1004-924X(2007)12-1900-08

同步辐射高分辨率衍射光束线的设计

U Pietsch[1]，O H Seeck[2]
（1. Faculty of Physics，Siegen University，D-57068 Siegen，Germany；
2. HASYLAB at DESY，D- 22603 Hamburg，Germany）

摘要：介绍了第三代同步辐射高分辨率 X 射线衍射光束线的总体设计。给出了高分辨率衍射的基本原理并描述了获得确定光子能量的近平行高强度 X 射线光束线所必需的光学元件。特别是用 X 射线动力学理论，解释了双晶及四次反射晶体单色器。作为一个实例，介绍了将于 2009 年开始在德国汉堡运行的一个新的同步辐射源 PETRAⅢ的高分辨率衍射（HighRes）光束线的设置情况。通过优化光学部件，对微米尺寸光束，q 空间的分辨减小到 $\Delta q=10^{-5}$ nm^{-1}，光通量大于 10^{11} cts/s。

关　键　词：同步辐射；衍射光束线；高分辨率
中图分类号：O434.19；O436.1　　**文献标识码：**A

Beam line design for high-resolution diffraction at synchrotron radiation sources

U Pietsch[1]，O H Seeck[2]

（1. *Faculty of Physics*，*Siegen University*，*D*-57068 *Siegen*，*Germany*；
2. *HASYLAB at DESY*，*D*- 22603 *Hamburg*，*Germany*）

Abstract：The general design of a high-resolution diffraction beamline at a third generation X-ray synchrotron radiation source is presented. For this，we introduce the basics of high resolution diffraction and the optical elements necessary to prepare a nearly parallel but intense X-ray beam with well-defined photon energy for high-resolution application. In particular，the function of double-crystal and four-bounced crystal monochromators is explained in terms of X-ray dynamical theory. As an example，we present the layout of the High Resolution Diffraction (HighRes) beamline at the new synchrotron radiation source PETRA III in Hamburg (Germany) which will become operational in 2009. By optimizing the optical components，a resolution in q-space will be achieved down to $\Delta q=10^{-5}$ nm^{-1} with micron beam size and a flux of more than 10^{11} cts/s.

Key words：synchrotron radiation source；diffraction beamline；high resolution

---

Received date：2007-08-20；**Revised date：**2007-10-10.

1 Introduction

In contemporary experimental science the radiation of modern synchrotron radiation sources is frequently used to investigate the properties of matter. For experiments with high photon flux but comparably large beam, the research centre DESY in Hamburg (Germany) is providing X-ray and VUV beams at the storage ring DORIS III. However, more and more experiments need micrometer-sized beams with very small divergence and high intensity (high brilliance). Coherence and well defined pulse structures are also much appreciated. To satisfy the increasing demand for this advanced beam properties, DESY is building up three new facilities: already operational is FLASH, a pulsed VUV free electron laser with extraordinary coherence and brilliance properties. In the planning phase is the XFEL, an X-ray free electron laser with comparable beam properties as FLASH but in the X-ray regime.

The new third generation storage ring for synchrotron radiation, PETRA III, is based on an existing storage ring structure which will be completely rebuilt for the purpose of synchrotron radiation[1]. It will deliver the most brilliant X-ray beam compared to other third generation sources in the world and becomes operational in early 2009. Nine sectors for X-ray and VUV experiments will be built up[2] and each sector will be equipped with either one long undulator (5 m or longer) or two 2 m undulators. The both 2 m undulators will be oriented not exactly in-line but slightly canted horizontally by 5 mrad. This canting angle is sufficiently large to install two completely independent beamlines in one sector. Sector 6 at PETRA III will house two beamlines for X-ray scattering and diffraction. One beamline is designed for Resonant Scattering and Diffraction (RSD) which will mainly be used for magnetic X-ray scattering experiments. The second beamline at the same sector is designed for High q-Resolution Diffraction (HighRes) and will deliver photons in an energy range from 5.4 keV up to 29.4 keV where the optics of the latter one is optimized for high q-resolution experiments.

2 Basics of high-resolution diffraction

The general layout of a high-resolution beamline is shown in Fig. 1. The main components of beamline optics are a pre-mirror and a monochromator. The function of the pre-mirror consists in removing the high energy part of the incidence spectrum. Considering refraction at the air-mirror interface, X-rays with energies smaller than the critical energy of total external reflection E_c will be reflected with nearly 100% whereas the intensities of those with higher energy rapidly decreases as E^{-4} due to Parratt's law[3]. As shown in Fig. 2, the cut-off energy decreases with increasing incidence angle, α_M, with respect to the mirror surface. In most cases α_M is set constant to define a spectral range sufficient for the experiment. The main optical element for high-resolution diffraction is the fixed-offset, double-crystal monochromator. It has two functions: first to maintain the general di-

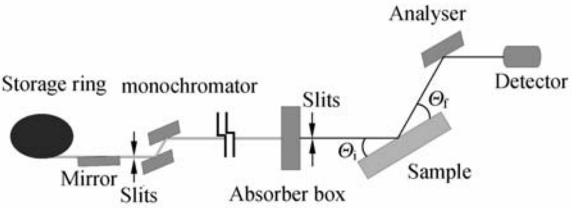

Fig. 1　General setup of a high-resolution diffractometer at a synchrotron beamline.

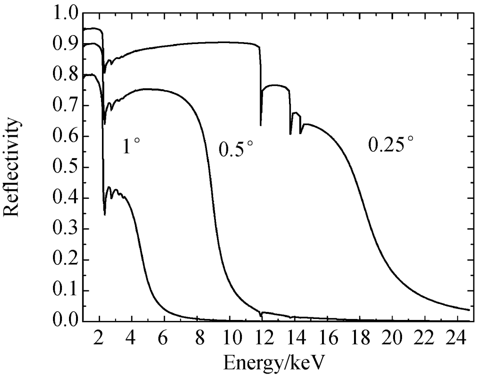

Fig. 2 Energy characteristics of a plane gold mirror for different incidence angles

rection of the beam pointing from the source to the experiment and second, to tailor the spectral width of the probing beam. Using dynamical theory, the full-width-half-maximum(FWHM), $\Delta\eta$, of X-ray diffraction from a perfect crystal is given by[4]

$$\Delta\eta=2C|\chi_h|\frac{1}{\sqrt{|b|}\sin(2\Theta_b)}\ , \tag{1}$$

where C is the polarization factor and b is the asymmetry factor which is a measure of the surface miscut of the crystal. The second essential quantity of dynamical diffraction is the Bragg angle shift. Due to refraction, the Bragg angle does not appear at the angular position obtained from the kinematical Bragg equation but is shifted by

$$\delta\eta=\frac{\chi_0}{2\sin(2\Theta_B)}(1-b)\ , \tag{2}$$

to higher angles. χ_0 in Eq. 2 and χ_h in Eq. 1 are given by

$$\chi_{0,h}=-\frac{\lambda^2}{\pi V}F(0,h)\ , \tag{3}$$

where the 0th and h th Fourier coefficients of the crystal polarizability depend on total electron density $F(0)/V$ and structure factor $F(h)$ of the crystal, respectively. λ is the wavelength. The asymmetry factor b is defined as

$$b=-\frac{\sin(\Theta_B+\phi)}{\sin(\Theta_B-\phi)}\ , \tag{4}$$

where ϕ is the angle between the diffracting lattice plane and the sample surface. Considering Eqs. 1,2 both the FWHM and peak position of the dynamical Bragg peak are functions of wavelength or energy, respectively. At certain wavelengths λ the FWHM of Si(111) is several times greater than the FWHM of its third harmonics, Si(333), scattering the at same angular range but with wavelength $\lambda/3$. At the same time the maxima of both Bragg peaks are slightly different in angular position. Therefore one can tune the monochromator angle to a value accepting λ only.

The angular acceptance $\Delta\eta$ of the Bragg reflection translates to a certain energy pass band. At a photon energy of 8 048 eV, which corresponds to a Bragg angle of $2\Theta_B=28.44°$, the pass band, given by $\Delta E/E=\Delta\eta/\Theta_B$ is 20×10^{-5} and 3.5×10^{-5} for Si (111) and Si (333), respectively.

The combination of two crystals into one unique optical element results in a double crystal arrangement. Assuming parallel setting of the two crystals of the same material and orientation, the so-called (+ −) setting is non-dispersive. Assuming the Bragg angles of both crystals, Θ_{B_1} and Θ_{B_2}, are equal, the second crystal accepts the same range of energy as accepted by the first crystal. The situation is visualised by a so-called DuMond diagram (Fig. 3)[5]. It shows the functional dependence of Bragg′s law for both crystals. The coordinate axes of both crystals are arranged to be parallel, but the horizontal (angular) axes are displaced by an angle β relative to each other, where β is the rotation angle of the second crystal with respect to the first one. At a given divergence of the incident beam, the whole energy range accepted by the first crystal is accepted by the second one as well. The intensity distribution of the double crystal arrangement as function of β is given by

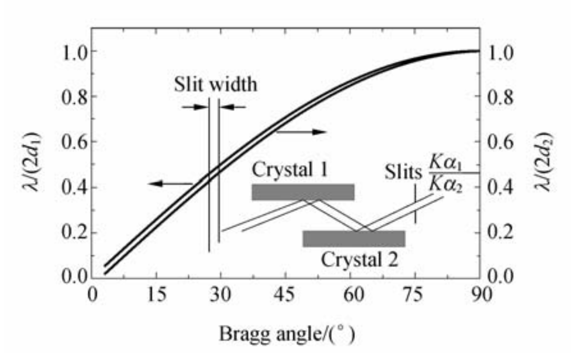

Fig. 3　DuMond diagram of a non-dispersive double crystal arrangement

$$I(\beta)=\int \mathrm{d}\eta_2 \mathscr{R}_1(\eta_1)\otimes \mathscr{R}_2(\eta_2)\ , \qquad (5)$$

where

$$\eta_2=\pm\left(-\frac{\eta_1}{b_1}+\beta\right)\ ,$$

is the angular deviation of the incidence angle at the second crystal. b_1 is the asymmetry factor of the first crystal. The ± sign refers to non-dispersive and dispersive arrangement, respectively. For a particular energy, the convolution product in Eq. 5 gives a reflection curve width of about $\sqrt{2}\ \Delta\eta$ as defined in Eq. 1 since both Bragg angles are equal.

A dispersive setting exits if $\Theta_{B_1}\neq\Theta_{B_2}$, either by use of two different Bragg reflections of the same crystal or two different crystal materials. Then both crystals diffract at a slightly different wavelengths which gives rise to a dispersion enlargement of the convoluted curve (Eq. 5) that can be approximated by

$$\Delta\eta(\Delta E)=\frac{\Delta E}{E}(\tan\Theta_1-\tan\Theta_2)\ . \qquad (6)$$

For synchrotron radiation sources this is almost automatically the case. Due to the heat load experienced by the first crystal its lattice spacing will differ from that of second crystal even for use of the same crystals and same Bragg diffraction. However, this effect can be minimized by cooling both crystals with liquid nitrogen.

A strictly dispersive arrangement is realized by an anti-parallel setting of both monochromator crystals. This (+ +) arrangement is shown in Fig. 4. The DuMond graphs of both crystals are aligned in opposite directions. Both branches overlap at one angle only. Since this overlap range in energy axes is smaller than the $\mathrm{K}\alpha_1$ — $\mathrm{K}\alpha_2$ separation of an X-ray tube, for example, the optical element would only accept one line. Thus this arrangement is mainly used for spectroscopic application.

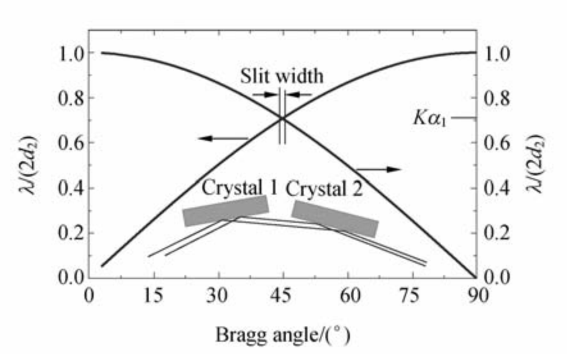

Fig. 4　DuMond diagram of a strict dispersive double-crystal arrangement

Both settings (+ +) and (+ —), respectively, are combined in four-reflection monochromators. It combines the advantage of low tail intensity of a (+ —) setting with the highly reduced energy band pass of the (+ +) arrangement. Additionally it maintains the incident beam direction. Four-bounced monochromators with fixed (022) or (044) crystal reflections are commercially available and are used in modern high-resolution diffractometers for laboratory application[6]. Four-reflection setups are also used at synchrotron sources.

For high-resolution application, it is useful to install an optical element in front of the detector and after the sample with similar optical properties as a monochromator. The acceptance of this analyser (see Fig. 1) can be tuned in a similar fashion as for a monochromator. In most cases a single crystal or a channel-cut crystal in (+ —) setting is sufficient.

The angular resolutions of the monochromator and analyser define a so-called resolution element in reciprocal space. If α_i and α_f are the incidence and exit angles of the beam with respect to the surface of the crystal under inspection, the resolution element is given approximately by $A_E = \delta Q_x \delta Q_z$, where

$$\begin{aligned} \delta Q_z &= K(\delta\alpha_f \cos\alpha_f - \delta\alpha_i \cos\alpha_i) + \\ &\quad \delta K(\sin\alpha_i + \sin\alpha_f) \\ \delta Q_x &= -K(\delta\alpha_i \sin\alpha_i - \delta\alpha_f \sin\alpha_f) + \\ &\quad \delta K(\cos\alpha_f + \cos\alpha_i) , \end{aligned} \qquad (7)$$

using $K = 2\pi/\lambda$. Because δQ_x and δQ_z change with α_i and α_f, both the size and shape of A_E will change during scanning of α_i and α_f[7]. Fig. 5 shows the shape of the resolution element in the vicinity of the Si(111) Bragg reflection of a float zone (FZ) silicon wafer. The streaks A and M are caused by the angular acceptance of the analyser and monochromator, respectively. The different extensions of both streaks are due to the use of a four-crystal monochromator but a single crystal as analyser. W denotes the wavelength streak reflecting the energy acceptance of the probed crystal. The resolution function A_E is convoluted with the scattering function of the crystal under investigation. Each feature of high intensity in a reciprocal space map will be accompanied by the appearance of M, A and W streaks. However, Fig. 5 shows that A_E becomes more circular in shape using four-bounced crystals at the monochromator and analyser site.

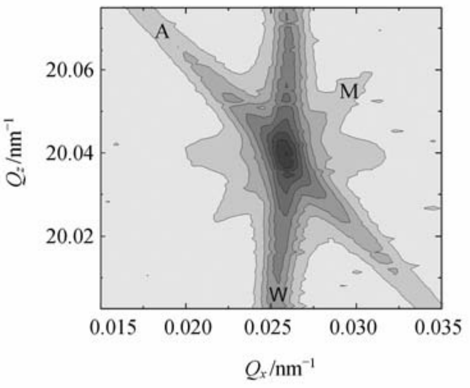

Fig. 5 Shape of the resolution element close to the Si(111) Bragg reflection of a FZ silicon wafer using a four-bounce monochromator and a plane single analyser crystal.

3 Design of HighRes beamline at PETRA III

The design of the HighRes beamline at PETRA III has to consider the following restrictions: (1) the optics should be designed for the highest possible q-resolution; (2) switching between a mode with a high-as-possible q-resolution and a relaxed mode in q-resolution should be possible; (3) the diffractometer and other equipment should be as accurate as possible; (4) vibrations should be avoided completely; and (5) as mentioned in the introduction, HighRes will share sector 6 with RSD which is a severe restriction in available space.

The last requirement strongly affects the design of the sector[8]. It burns out that the 5 mrad natural separation of the two undulators is too small for two diffraction beamlines, as the diffractometers and the experimental equipment need a lot of space in all directions. Therefore it was decided to offset the beamline HighRes vertically by 1.25 m from the floor level of the beamline RSD (without vertical offset). This design is justified by the scientific case of RSD where the photon energy ranges is scanned frequently in an energy range of 2.5 keV up to 50 keV which is not possible on an offset beamline.

A schematic of the beamline design is shown in Fig. 6. The decision to vertically offset HighRes has direct consequences for the design of the optics. A fixed offset of 1.25 m and an energy range of 5.4 keV up to 29.4 keV, as mentioned in the introduction, can only be realized with a fixed offset double monochromator the so-called Large Offset Monochromator (LOffsMono). The stability of the LOffsMono should be has high as possible. Therefore, a liquid nitrogen cooled double crystal Si(111) pre-monochromator (liqN2Mono) will be installed to minimize the heat load on the LOffsMono. Also, the length of the LOffsMono should be restricted to 3 m. Thus, Si(311) (5.4～18.4 keV) and Si(511) (8.4～29.4 keV) are selected as monochromators. Compared to the Si(111) of the liqN2Mono the Si(311)/Si(511) reflections are less intense but better defined in phase space which is required to achieve high *q*-resolution. Therefore, the LOffsMono at the same time serves as a high *q*-resolution element and as a beam offsetting device.

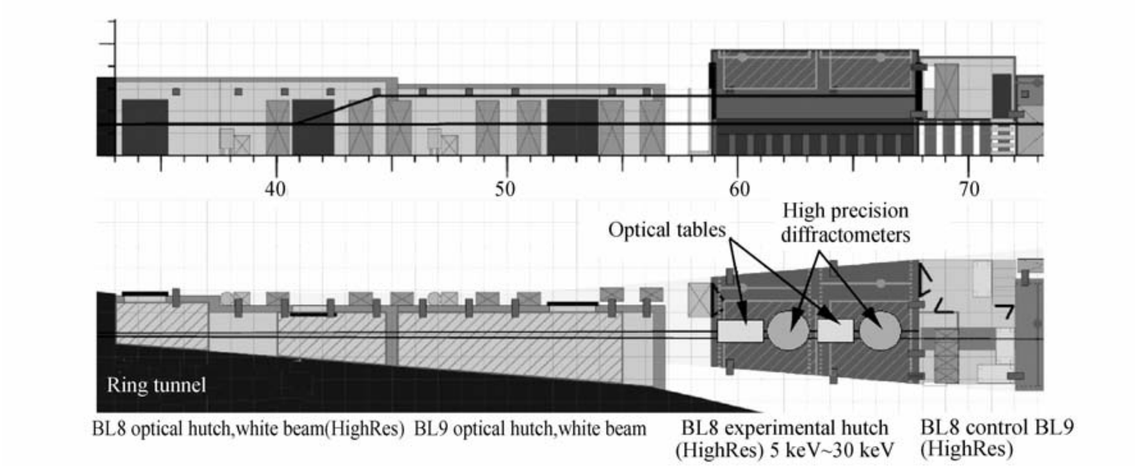

Fig. 6　Principal design at sector 6 of PETRA III hosting two different experiments. The HighRes beamline experiences a vertical offset of 1.25m realized by two double crystal monochromators.

Figs. 7 and 8 show the DuMond diagrams of both possible configurations of the liqN2Mono and the LOffsMono. If the first both crystals scatters down and the second ones scatter up (Fig. 7). One has the (− +)(+ −) setup mentioned above and which is usually used for high-resolution optics. If both twins, i. e. liqN2Mono and LOffsMono, scatter up, it defines a (+ −)(+ −) setup which is usually not used (Fig. 8). However, in the case of the HighRes beamline the second setup combines high resolution with the geometric requirement of beamline construction. Due to the 2 km circumference and the source height of only 20 μm PETRA III will provide an X-ray beam with very low vertical divergence (the grey bars in Figs. 7 and 8). Therefore both setups are almost identical in performance for zero-order photon energy (10 keV, for examples). Both setups differ in capability to reject higher harmonics. For the (− +)(+ −)-setup the relevant 3rd-order Bragg peak is located very close to the zero-order Bragg peak and its reflectivity is suppressed by 3

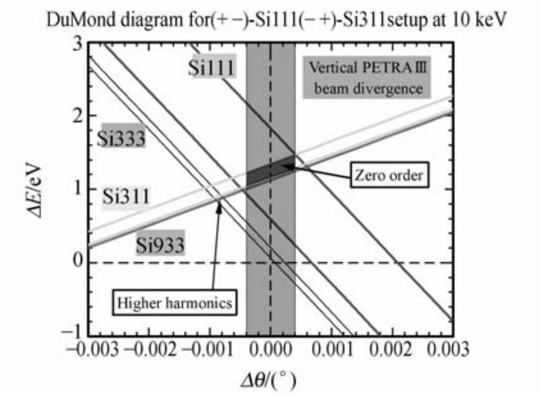

Fig. 7　DuMond diagram of a possible setup of two double crystal monochromators in (− +)(+ −) arrangement. The angular width of the incident beam is marked in grey.

~4 orders of magnitude only. At the (+ −)(+ −)-setup the 3rd order Bragg peak is far off the zero-order Bragg peak and its intensity is 8~9 orders of magnitude below the zero order intensity, i. e. suppression of higher harmonics is almost complete. Due to this nearly complete rejection of higher harmonics X-ray mirrors are not needed at HighRes. Instead, compound refractive lenses (CRL) can be used to focus or collimate the beam. CRLs have certain advantages over mirrors as they are easier to install and to handle (in-line optics) and are also less sensitive to vibrations and mechanical stress.

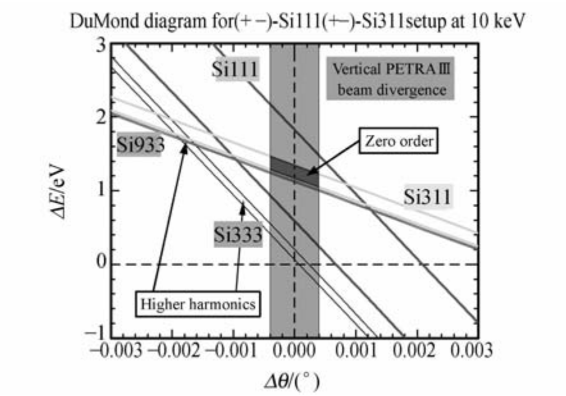

Fig. 8 DuMond diagram of a possible setup by two subsequent double crystal monochromators in (+ −)(+ −) arrangement. The angular width of the incident beam is marked in grey.

Three different modes will be available by default: the "raw mode" is relaxed in q-resolution but delivers the most intense beam. In the "collimating mode" the q-resolution is exceptionally good but at the expense of slightly reduced intensity . The " focussing mode " creates a micrometer beam spot at the sample with a q-resolution comparable to the "raw mode". The intensity of the full beam at the sample will be from 1×10^{11} ph/s up to 5×10^{12} ph/s depending on the photon energy and the selected mode. The higher harmonics suppression will be almost complete. The experimental hutch will be equipped with a high precision multi-circle diffractometer and two motorized optical tables. There is additional space for a second diffractometer (to be installed in a later phase) or other user-defined experimental setups, such as a liquid scattering add-on. The achievable resolution in q space will be $\delta Q_z = 5\times10^{-5}$ nm^{-1} and $\delta Q_x = 2\times10^{-5}$ nm^{-1} which is one order of magnitude better than any beamline up to now.

In summary, the HighRes beamline will deliver an extreme stable X-ray beam with almost complete higher harmonic suppression and the choice of focusing or collimation. The experimental equipment will match the beam properties so that experiments with very high stability and highest q-resolution will be possible. These experimental conditions are best for investigation of highly perfect crystalline materials and for artificial or self organized structures up to micrometer size range.

4 Acknowledgement

The authors thanks The Sino-German Center for Research Promotion for support.

References:

[1] FRANZ H, LEUPOLD O, HLSBERGER R R, *et al*.. PETRA III: DESY's new high brilliance third generation synchrotron radiation source[J]. *Synch. Rad. News*, 2006, 6:25-29.

[2] BALEWSKI K, BREFELD W, DECKING W, *et al*.. *PETRA III: A Low Emittance Synchrotron Radiation Source* [M]. DESY Press, 2004.

[3] PARRATT L G. Surface studies of solids by total reflection of X-rays[J]. *Phys. Rev.*, 1954, 95(2): 359-369.

[4] PINSKER Z G. Dynamical scattering of X-rays in crystals[J]. *Springer*, 1978.

[5] DUMOND J W M. Theory of the use of more than two successive X-ray crystal reflections to obtain increased resolving power[J]. *Phys. Rev.*, 1937, 52(8): 872-883.

[6] BARTELS W J. Characterization of thin layers on perfect crystals with a multipurpose high resolution X-ray diffractometer[J]. *J. Vac. Sci. Technol.*, 1983, B1: 338-345.

[7] PIETSCH U, HOLY V, BAUMBACH T. High-resolution X-ray scattering from thin films and lateral nanostructures[J]. *Springer*, 2004.

[8] BUNK O. High resolution X-ray diffraction beamline[P]. *PETRA* Ⅲ *Technical Design Report*, 2003.

Authors' biographies: **Ulrich Pietsch** graduated in crystallography in 1978 and received his PhD in 1981 and habilitation in 1988 in experimental physics from the University of Leipzig. Since 2005 he has been a professor of Structural Solid State Physics at Siegen University and is interested in high-resolution X-ray diffraction studies of thin films and lateral nanostructures. E-mail: pietsch@physik.uni-siegen.de

Oliver Seeck received his PhD in physics in 1997 from the University of Kiel. Since 1999, he has worked on synchrotron radiation sources investigating surfaces and thin films. Currently, he is responsible for the design of a High Resolution Diffraction Beamline at PETRA III, Hamburg (Germany).